

## Phase homogeneity and crystal morphology of the malaria pigment $\beta$ -hematin

D. Scott Bohle<sup>a\*</sup>, Andrew D. Kosar<sup>a</sup> and Peter W. Stephens<sup>b</sup>

<sup>a</sup>Department of Chemistry, University of Wyoming, Laramie, Wyoming, 82071-3838, United States of America, and

<sup>b</sup>Department of Physics, State University of New York, Stony Brook, Stony Brook, New York, 11794-3800, United States of America. E-mail: Bohle@uwyo.edu

Hemoglobin digestion in the intraerythrocytic trophozoite stages of the malaria parasite releases large quantities of heme, which is then detoxified by crystallization into regular crystallites, which are subsequently secreted into the host vascular network as malaria pigment. This crystalline product is isostructural with the synthetic phase  $\beta$ -hematin, and its structure, solved from its powder diffraction pattern, (Pagola *et al.*, 2000), corresponds to a hydrogen bonded chain of propionate linked dimers, Figure 1. This is an example where the crystalline phase is the macromolecule of direct biological interest, particularly in light of the currently accepted hypothesis for the quinoline antimalarial drug action being the inhibition of  $\beta$ -hematin formation and biosynthesis. A surprisingly array of spectroscopically similar closely related phases can also form during the reactions which are used to synthesize  $\beta$ -hematin. Scanning electron microscopy and X-ray powder diffraction have been used to characterize these materials. Taken together these

results indicate that infrared spectroscopy, in itself, is insufficient to identify synthetic analogs to malaria pigment and that a combination of electron microscopy and powder diffraction are required to unambiguously characterize these heme aggregates.

**Keywords:** malaria pigment, morphology, structure

### 1. Introduction

Following invasion of red blood cells by the merozoite stages of *plasmodia*, hemoglobin from the host cell is imported into a digestive vacuole of the parasite (Collins & Paskewitz, 1995). Within this vacuole an organized set of processes strip the heme from the peptide, oxidize it, nucleate its crystallization, and then aggregate it into the crystalline material termed malaria pigment or hemozoin (Olliaro & Goldberg, 1995). Although we now have an excellent understanding of the peptide degradation of the globin (Gluzman *et al.*, 1994; Francis *et al.*, 1997), heme processing, and its relationship to peptide degradation, remains poorly understood.

As part of our project to understand heme detoxification by *plasmodia* we have demonstrated that the synthetic phase  $\beta$ -hematin is crystallographically identical to malaria pigment, (Bohle *et al.*, 1997), and that it consists of hydrogen bonded chains of heme dimers where the heme are reciprocally linked by propionate side-chains hemes, Figure 1, (Pagola *et al.*, 2000). Although the infrared signature for  $\eta^1$ -propionate Fe-O bond formation was recognized in early studies of the synthetic phase  $\beta$ -hematin, and isolated and purified malaria pigment, (Slater *et al.*, 1991), prior authors

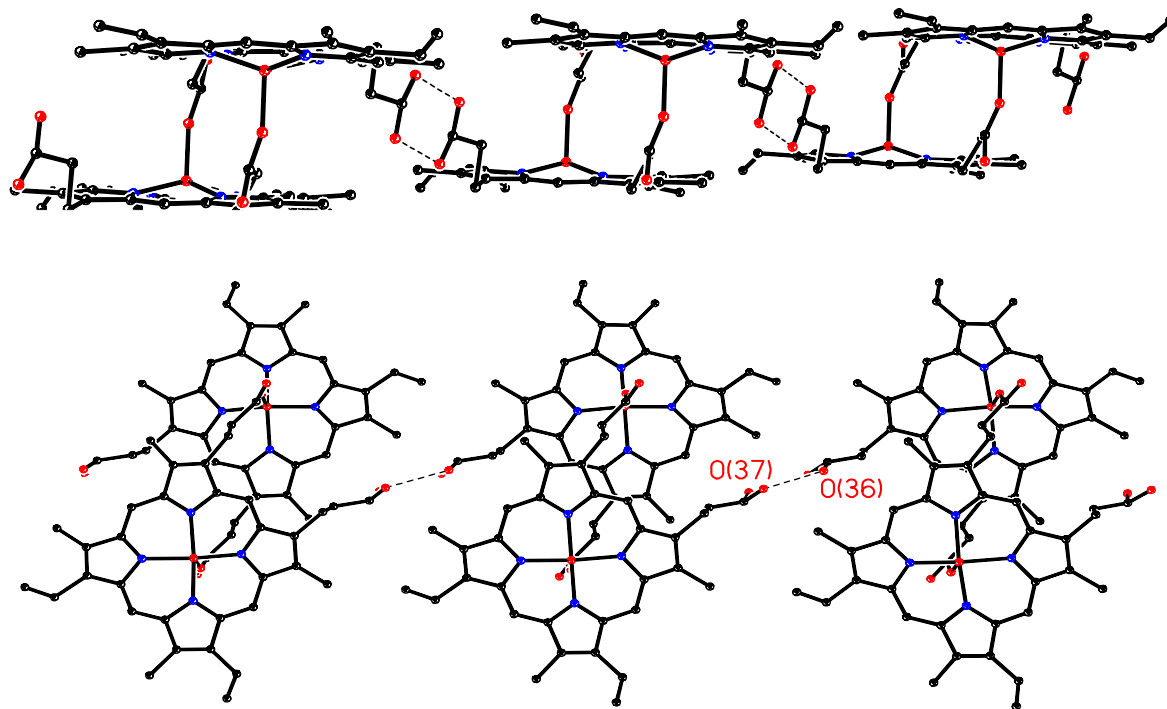


**Figure 1**

Two views of the structure of  $\beta$ -hematin determined by solution of the X-ray powder diffraction pattern. Both views show the iron-oxygen and propionic acid linkages between dimeric pairs of hemes. The five coordinate high spin iron,  $S = 5/2$ , is located 0.47 Å out of the plane of the porphyrin and forms a relative short bond, 1.889(2) Å, with one of the oxygens of the paired protoporphyrin-IX propionic acid substituents. The full heme framework is shown in Figure 2.

attributed its profound insolubility to a putative heme polymerization of propionate linked hemes, (Slater & Cerami, 1992). The structure in Figure 1 was determined by Monte Carlo, simulated annealing, and Rietveld techniques for powder diffraction data measured for synthetic  $\beta$ -hematin. In this case the synthetic  $\beta$ -hematin was prepared under anhydrous conditions in the presence of coordinating solvents which slow crystal growth and result in homogenous products consisting of a single phase which gives outstanding powder diffraction patterns. Nevertheless, crystallite size from these and other preparations have so far limited X-ray diffraction experiments to non-oriented powder samples. In this paper we illustrate some of the morphological and diffraction characteristics for samples of  $\beta$ -hematin prepared by rapid precipitation methods.

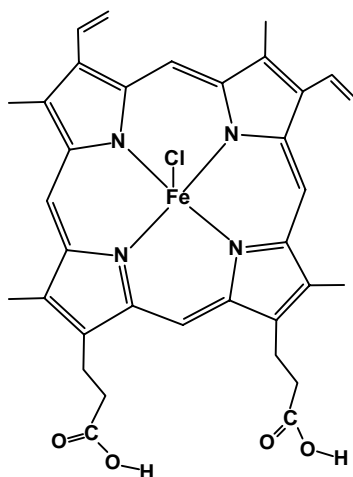
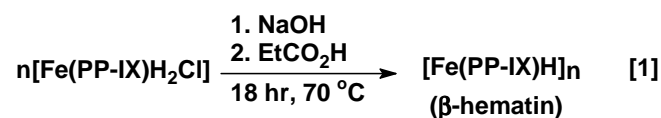


**Figure 2**  
The structure of iron(III)(protoporphyrin-IX)Cl.

## 2. Materials and methods

### 2.1 Synthesis

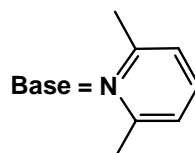
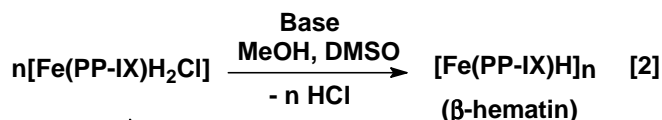
#### *Aqueous acid-catalyzed method, Equation 1.*



Following published methods of preparation (Slater *et al.*, 1991),  $\alpha$ -hematin is dissolved in 0.1 M sodium hydroxide with stirring for 30 min. It is then brought to acidic condition with slow addition of propionic acid. It was then stirred at 70° C for 18 hours. The solution and precipitate were allowed to stand and the aqueous solution was decanted off. The solid was then washed with distilled water and again decanted off the solution. This was repeated three times with methanol washes between each water wash. The solid was then washed with 0.1 M sodium bicarbonate solution (pH 9.1) for 3 hours. The solution was decanted off and the solid was collected on a 10- 20  $\mu\text{m}$  sintered glass frit. It was again washed with distilled water and methanol. The solid was dried *in vacuo* over phosphorus pentoxide over night. Infrared analysis has bands at 1210  $\text{cm}^{-1}$ , 1663  $\text{cm}^{-1}$ , and 1711  $\text{cm}^{-1}$ . Elemental analysis is in

good agreement with the previously published results for this method (Analyzed: C, 64.7 %; H, 5.0 %; N, 8.7 %. Found: C, 64.47 %; H, 5.17 %; N, 8.83 %). Typical yields for this method are 94-98%.

#### *Anhydrous non-coordinating-base method, Equation 2.*



This is a modification of the literature preparation [Bohle, 1993 #338]. In an inert atmosphere, hemin is dissolved in a minimal amount of 2,6-lutidine with stirring. Upon completion of the dissolution, a 50:50 mixture of anhydrous methanol: dimethyl sulfoxide was added and the flask was sealed and protected from moisture and ambient light. The flask was then removed from the inert atmosphere and was allowed to stand undisturbed for two weeks to several months. After the allotted time, the solution was filtered and the black solid was collected on a 10- 20  $\mu\text{m}$  sintered glass frit. The solid was rigorously washed with methanol (2 x 10 ml), a 0.1 M sodium bicarbonate solution (pH 9.1) (4 x 30 ml), and distilled water (2 x 20 ml) after which the filtrate ran clear. The solid was dried in an oven at 150° C overnight. IR analysis has characteristic bands at 1210  $\text{cm}^{-1}$ , 1664  $\text{cm}^{-1}$ , and 1711  $\text{cm}^{-1}$ . Elemental analysis for this preparation was in good accord with previously reported results (Analyzed: C, 64.71 %; H, 4.92 %; N, 8.69 %. Found: C, 64.95 %; H, 5.21%; N, 8.93 %). Typical yields afford 80- 97 % conversion.

### 2.2 Physical methods

**2.2.1. Low resolution X-ray powder diffraction.** Low resolution X-ray powder diffraction (XRD) were collected using Cu  $K_\alpha$  radiation ( $\lambda = 1.54059 \text{ \AA}$ ) on an XDS 2000 X-ray Diffractometer. Data was processed with DMS 2000 v.2.45 Data Management System (Scintag, 2000)

**2.2.2. High resolution X-ray powder diffraction.** A synchrotron radiation source, at Beamline X3B1 of the National Synchrotron Light Source at the Brookhaven National Laboratories was used for high resolution X-ray powder diffraction. Wavelength calibration was performed with  $\text{Al}_2\text{O}_3$  standards.

**2.2.3. Scanning electron microscopy.** Scanning electron microscopy (SEM) experiments were conducted using a JEOL model JSM 5800-LV Scanning Electron Microscope fitted with an EDS detector. Operating conditions were an accelerating voltage of 20,000 eV. In order to avoid the necessity of applying a conductive coating to the samples, backscattered electron images were acquired while operating the microscope in a low vacuum mode. Typical vacuum conditions for image acquisition were 20 Pa in the sample chamber. Image and spectra processing were done using Voyager Version 2.4, running on a SUN Workstation (Middleton).

### 3. Results and discussion

The standard synthesis of  $\beta$ -hematin, equation 1, superficially resembles malaria pigment in the parasites acidic digestive vacuole

in that acidic conditions are employed during the precipitation/aggregation step. However both the initial steps, and subsequent purification steps illustrate some of the significant problems associated with this synthesis. Although monomeric

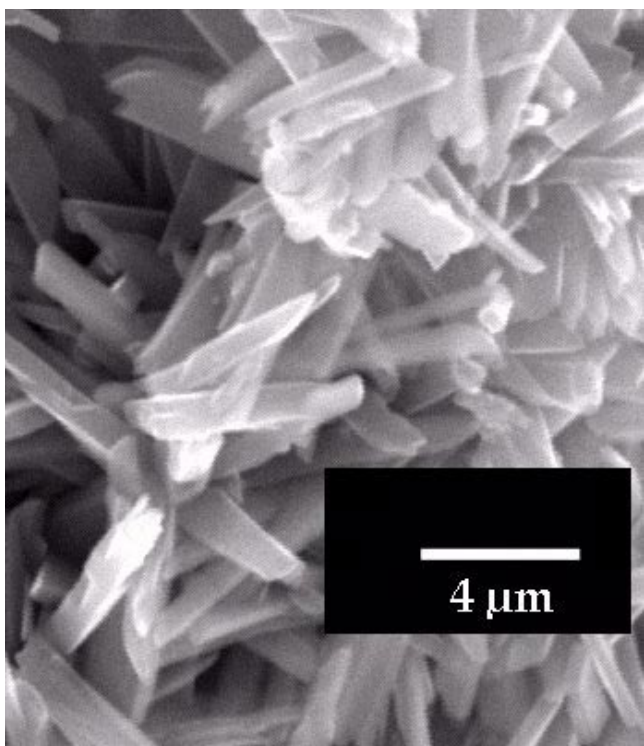
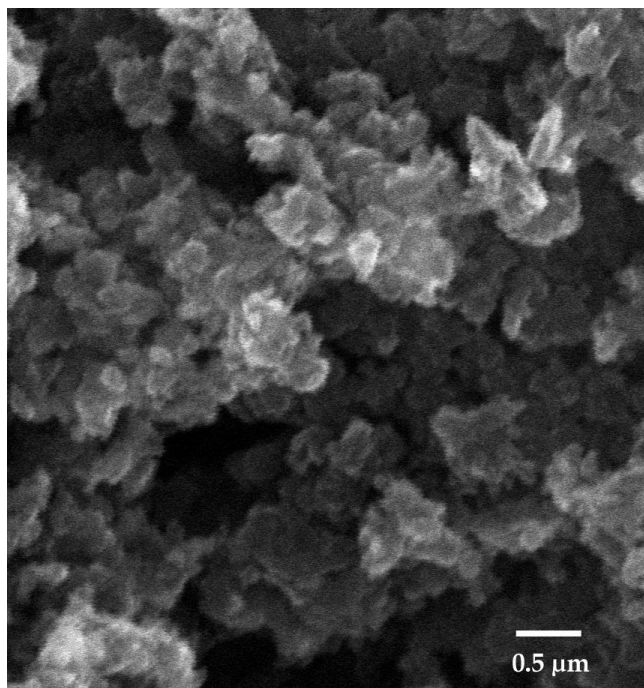
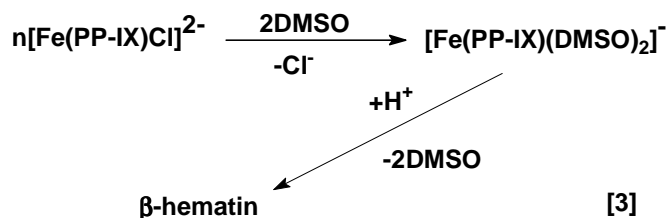


**Figure 3**  
SEM images of (top)  $\beta$ -hematin produced by the reaction in equation 1, and (bottom) by equation 2.

hemin,  $\text{Fe(III)(PP-IX)Cl}$ , is used as the starting material, it is dissolved in 0.1 M sodium hydroxide and then precipitated with propionic acid before annealing at 70 °C. During this dissolution step the oxo-bridged dimer,  $(\text{PP-IX})\text{Fe(III)-O-Fe(III)(PP-IX)}$  rapidly forms, and it will be a significant component of the initial acid precipitate. Although the buffered acid conditions used in the annealing will result in acid mediated oxo-bridge cleavage, to give hemin, this relatively slow transformation is likely not to be that found in the parasite since  $\text{Fe(II)(PP-IX)}$  is the most likely initially released form of heme. Although it can be activated to bind oxygen, and auto-oxidize to give  $(\text{PP-IX})\text{Fe(III)-O-Fe(III)(PP-IX)}$  after four steps, two of which are bimolecular in heme (Alben, 1968; Hammond & Wu, 1968), there is no evidence for the presence of this complex either in the isolated product or in the digestive vacuole *in situ*. Moreover, there are a variety of other pathways by which  $\text{Fe(II)(PP-IX)}$  can potentially be oxidized, among which is direct outer-sphere electron transfer. Clearly in terms of either the starting heme complex, its concentration, its form, or its identity the reaction shown in equation 1 does not correspond to the parasite's biosynthesis. Equally significant is the requirement for the products from equation 1 to be subject to extensive repeated washes with pH = 9 bicarbonate solutions. Whereas these washes remove a considerable amount of poorly aggregated heme from the product of equation 1, this step dissolves little heme from malaria pigment itself, nor from the products from equation 2.



More crystalline samples of  $\beta$ -hematin result when the crystallization is slowed down and completely soluble precursors and complexes are employed. The method we have devised to achieve this (Bohle *et al.*, 1994) is to use organic solvents to solubilize and co-ordinate the heme, and then employ the non-coordinating base 2,6-dimethylpyridine (2,6-lutidine) to abstract HCl to form the aggregated phase. Thus the solvolysis in equation 3 is established and this has the net effect of slowing down the crystallization of  $\beta$ -hematin from these solutions. Significantly, although the infrared spectra of the products from equations 1 and 2 are spectroscopically identical, (Bohle & Helms, 1993), we show in this paper that there are major differences in the diffraction and morphological features of the precipitates. It is critical however to ensure that all reagents in these reactions are completely anhydrous to avoid base mediated formation of the oxo bridged dimer.

Scanning electron microscopy, Figure 3, illustrates the marked differences in morphology of the products of equations 1 and 2. As can be seen in Figure 3(top), the crystallites from the acid precipitation reaction, equation 1, have few distinguishable facets and have an upper estimate of 0.2  $\mu\text{m}$  for the largest visible crystal dimension. Similar SEM images for preparations of this type have also recently been published (Egan *et al.*, 1999). In contrast the crystallites resulting from the base mediated reaction in equation 2, Figure 3(bottom), have maximum lengths ca. 20 fold larger. More significantly however, they have very regular morphologies and sizes throughout the sample. The crystallites in Figure 3(bottom) are also similar to published images (Sullivan *et al.*, 1996b) of those formed by the parasite in width and thickness, but not in length.

The digestive vacuole of the parasite is only ca. 3  $\mu\text{m}$  in diameter, and typical malaria pigment crystallites are only 1  $\mu\text{m}$  long. The corresponding diffraction results for these phases are shown in Figure 4.

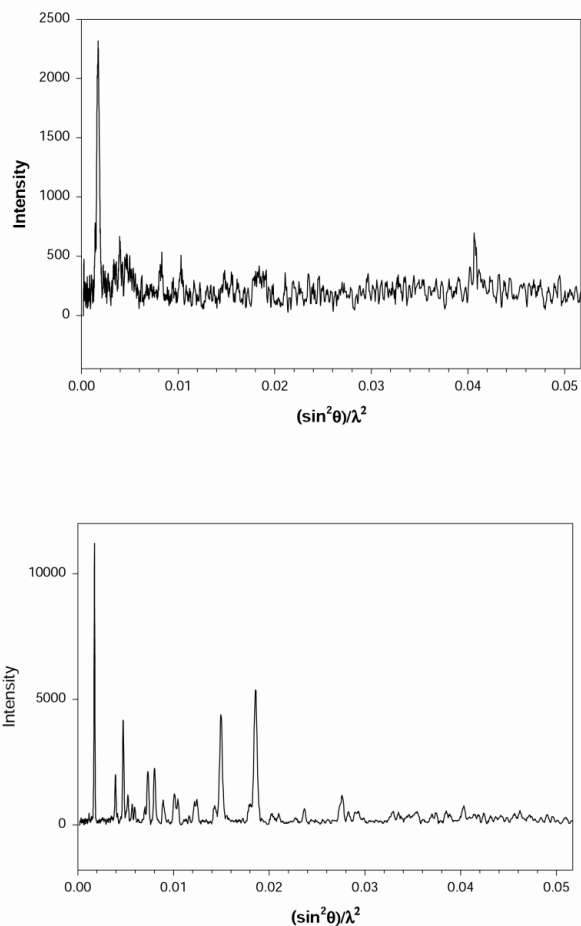


**Figure 4**  
Powder diffraction patterns for (top)  $\beta$ -hematin prepared by the reaction in equation 1, and (bottom) by equation 2. Diffraction data, corresponding to  $2 - 41^\circ$  in  $2\theta$ , measured with  $\text{CuK}\alpha_1$  radiation.

Both diffraction patterns are dominated by the intense [100] reflection at  $\sim 7^\circ$  in  $2\theta$ , but the crystallinity of the material from the preparation in equation 2 is much higher. One consideration for the differences in the quality of the diffraction patterns in Figure 4 is that there is a clear difference in particle size from their corresponding SEM images in Figure 3. In support of this observation is that the full width half maximum for the two patterns are  $0.62^\circ$  and  $0.18^\circ$  respectively. In addition to the particle size effects, other samples of  $\beta$ -hematin prepared by the acid precipitation method give new peaks near the [100] line, ranging from simple splitting, as in Figure 5 (middle), to multiple new lines in this region, as shown in Figure 5 (bottom). We have not yet been able to determine the lattices of the phases responsible for these new diffraction lines as all attempts to index the small number of sharp lines have failed to give a unique unit cell with all lines indexed. In addition many of the lines in the bottom trace in Figure 5 are very broad and weak.

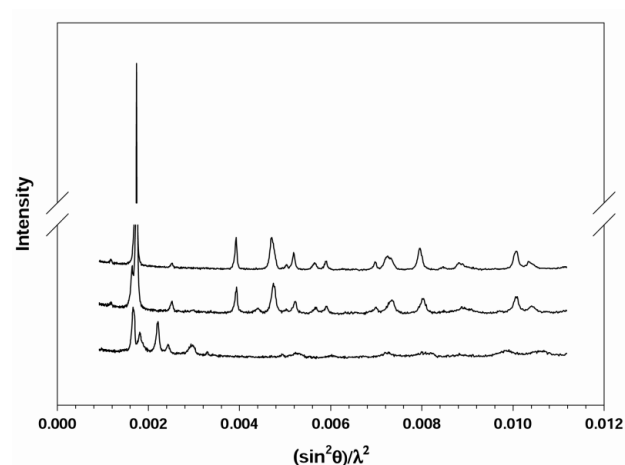


**Figure 5**  
X-ray powder diffraction traces for three preparations of  $\beta$ -hematin. Top trace corresponds to product of equation 2, while those in the middle and bottom traces show two different samples prepared from equation 1. Data measured on beamline X3B1  $\lambda = 1.15095 \text{ \AA}$ , correspond to  $4 - 11^\circ$  in  $2\theta$ .

A variety of macromolecules have been proposed to catalyze, initiate, or mediate heme aggregation in malaria. Among these are the family of unusual histidine rich protein, HRP I-IV, (Sullivan *et al.*, 1996a; Choi *et al.*, 1998) which bind large quantities of heme. In addition, glycoproteins and lipids have been suggested to mediate malaria pigment formation (Arese *et al.*, 1999; Fitch *et al.*, 1999). Clearly the reactions outlined in equation 1 and 2 can generate aggregated heme phases without catalysis, but the role of macromolecular catalysis of these reactions remains an important research effort. The results in this paper illustrate that the heme aggregates which are precipitated by these systems need to be carefully scrutinized, especially by powder diffraction, to ensure that they are malaria pigment and not some other insoluble phase.

#### 4. Conclusions

While many spectroscopic methods provide insight into the nature of the bonding and structure of the individual heme centers in  $\beta$ -hematin, they have not allowed for distinctions in the nature of the aggregated phase (Bohle *et al.*, 1994; Bohle *et al.*, 1998). These distinctions can be either chemical, in the form of differential solubility in bicarbonate solutions, morphological, in the form of different crystal sizes, or crystallographic, in terms of how they diffract X-rays. Malaria produces crystals with remarkably uniform morphology and size (Sullivan *et al.*, 1996b; Egan *et al.*, 1999) and these resemble those produced by the reaction in equation 2. Although the abstraction of HCl is not the reaction which takes place in the parasite's digestive vacuole, the resulting phase is similar to the natural malaria pigment.

Many questions are raised by the structure in Figure 1. Among the critical areas for which answers are urgently needed, are at what stage do the propionate linked dimers form; how is the heme oxidized, and what is the active growing surface of the crystal to which the antimalarial drugs bind to? Our studies to answer these and related questions are in progress.

We would like to gratefully acknowledge support for this research by the World Health Organization and by the Burroughs Wellcome fund in the form of a New Initiatives in Malaria grant to DSB and PWS.

### References

- Alben, J. O. (1968). *Biochemistry*, **7**, 624-635.
- Arese, P., Schwarzer, E., Giribaldi, G., Ulliers, D., Valente, E. & Ludwig, P. (1999). *J. Leukocyte Biol.* (SS), 129.
- Bohle, D. S., Conklin, B. J., Cox, D., Madsen, S. K., Paulson, S., Stephens, P. W. & Yee, G. T. (1994). *ACS Symposium Ser.* **572**, 497-515.
- Bohle, D. S., Debrunner, P., Jordan, P. A., Madsen, S. K. & Schulz, C. E. (1998). *J. Am. Chem. Soc.* **120**, 8255-8256.
- Bohle, D. S., Dinnebier, R. E., Madsen, S. K. & Stephens, P. W. (1997). *J. Biol. Chem.* **272**(2), 713-716.
- Bohle, D. S. & Helms, J. B. (1993). *Biochem. Biophys. Res. Commun.* **193**(2), 504-508.
- Bohle, D. S., Helms, J. B., Pfeifer, C. A. & Smith, B. D. (1993). *Abstracts of Papers of the American Chemical Society*, **205**(Pt1), 503-INOR.
- Choi, C. Y. H., Cerda, J., Babcock, G. T. & Marletta, M. A. (1998). *Abstracts of Papers of the American Chemical Society*, **216**(Pt1), 48-BIOL.
- Collins, F. H. & Paskewitz, S. M. (1995). *Annu. Rev. Entomol.* **40**, 195-219.
- Egan, T. J., Hempelmann, E. & Mavuso, W. W. (1999). *J. Inorg. Biochem.* **73**(1-2), 101-107.
- Fitch, C. D., Cai, G. Z., Chen, Y. F. & Shoemaker, J. D. (1999). *Biochim. Biophys. Acta-Mol. Basis Dis.* **1454**(1), 31-37.
- Francis, S. E., Sullivan, D. J. & Goldberg, D. E. (1997). *Annu. Rev. Microbiol.* **51**, 97-123.
- Gluzman, I. Y., Francis, S. E., Oksman, A., Smith, C. E., Duffin, K. L. & Goldberg, D. E. (1994). *J. Clin. Invest.* **93**(4), 1602-1608.
- Hammond, G. S. & Wu, C.-S. (1968). *Adv. Chem. Ser.* **77**, 186-207.
- Olliaro, P. L., Goldberg, D. E. (1995). *Parasitol. Today*, **11**(8), 294-297.
- Pagola, S., Stephens, P. W., Bohle, D. S., Kosar, A. D., Madsen, S. K. (2000). *Nature*, **404**, 307-310.
- Scintag (2000). DMS 2000 Data Management System. Sunnyvale, CA.
- Slater, A. F. G. & Cerami, A. (1992). *Nature* **355**(6356), 167-169.
- Slater, A. F. G., Swiggard, W. J., Orton, B. R., Flitter, W. D., Goldberg, D. E., Cerami, A. & Henderson, G. B. (1991). *Proc. Natl Acad. Sci. USA*, **88**(2), 325-329.
- Sullivan, D. J., Gluzman, I. Y. & Goldberg, D. E. (1996a). *Science* **271**(5246), 219-222.
- Sullivan, D. J., Gluzman, I. Y., Russell, D. G. & Goldberg, D. E. (1996b). *Proc. Natl Acad. Sci. USA*, **93**(21), 11865-11870.